

COMPARISON OF THE UNITED STATES PRECISION LIGHTNING NETWORK™ (USPLN™) AND THE CLOUD-TO-GROUND LIGHTNING SURVEILLANCE SYSTEM (CGLSS-II)

Alexander A. Jacques, James P. Koermer*, and Thomas R. Boucher
Plymouth State University, Plymouth, NH

1. INTRODUCTION

WSI Corporation (WSI) requested a comparative study of their United States Precision Lightning Network™ (USPLN™), co-owned by WSI and TOA Systems, Inc., with another lightning detection network. The USPLN is a nationwide network that consists of over 100 sensors dispersed across the continental United States (CONUS). With global expansion, the network is now a subset within the growing Global Lightning Network® (GLN®). The network was first developed by TOA Systems, Inc. and Weather Decision Technologies (WDT), Inc. as an alternative to the widely-recognized National Lightning Detection Network (NLDN). After testing, the USPLN began operations in 2004. In 2007, WSI acquired the share of the network owned by WDT, Inc. and began the expansion project for the GLN in 2008. At the present time, over 160 sensors cover the North American continent alone (Neilley and Bent 2009). Figure 1 displays the locations of the nine USPLN sensors covering the state of Florida, which is the primary location for this study.

Previous evaluations of USPLN performance metrics have been limited to simulations and individual case study analyses. A numerical simulation of the network was conducted by randomly distributing cloud-to-ground (CG) strokes across the CONUS. Using the USPLN sensor characteristics, the expected signal response and location procedures were processed as if they were real strokes. Network simulation results produced average stroke detection efficiencies (DE) of over 95% across the majority of the CONUS. A mean location error of less than 250 m was also determined through this network simulation (Neilley and Bent 2009). Case studies involved examination of fixed tower locations. During the summer of 2008, eight strokes were detected by the USPLN within a

600 m radius of a 549 m tall tower near Miami, FL. Assuming that all of these strokes struck the tower itself, the calculated mean location error of the eight strokes was 186 m (Neilley and Bent 2009). Outside of these simulation and case study analyses, a longer-term evaluation of USPLN performance had not been conducted. This project attempts to partially achieve that goal.

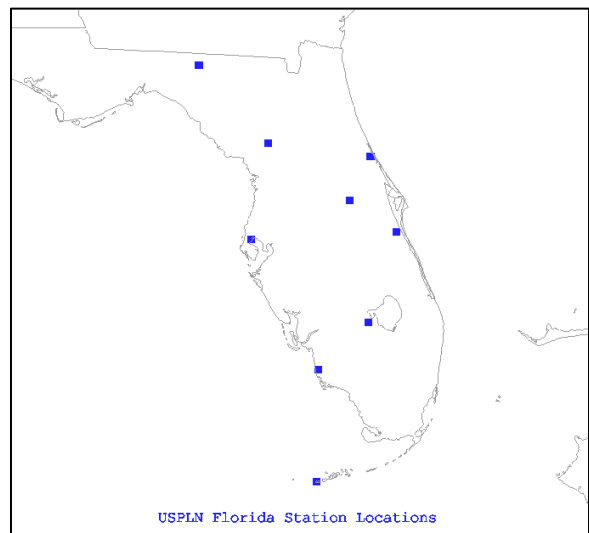


Figure 1. Locations of the nine USPLN sensors stationed in Florida.

A simple method to evaluate performance of a lightning detection network over an extended time period is to compare it with another lightning detection network with well-established performance metrics. The additional network utilized in this study is the second generation of the Cloud-to-Ground Lightning Surveillance System (CGLSS-II). CGLSS-II is a local NASA and Air Force detection network consisting of six sensors, displayed in Figure 2, surrounding the Kennedy Space Center and Cape Canaveral Air Force Station (KSC/CCAFS). The network was renamed CGLSS-II after CGLSS-I received a processor upgrade in 2008, which allowed for CGLSS-II to resolve all stroke locations in real time, whereas CGLSS-I could only process flashes (Flinn *et al.* 2010). The CGLSS-II network has been a certified system by the United States Air Force since 1989, and is utilized by the

*Corresponding author address: James P. Koermer, Department of Atmospheric Science and Chemistry, Plymouth State University, MSC #48, 17 High Street, Plymouth, NH, 03264; e-mail: koermer@plymouth.edu

45th Weather Squadron (45 WS) for all lightning detection procedures at KSC/CCAFS (Boyd *et al.* 2005). These procedures include lightning advisory issuance, Lightning Launch Commit Criteria (LLCC) evaluation, and inspections to launch payloads for possible induced current damage by direct or nearby hits (Flinn *et al.* 2010; McNamara *et al.* 2010). The importance of these safety procedures, combined with KSC/CCAFS being located in an area of high annual lightning flash density, require CGLSS-II to carry strong performance metrics (Huffines and Orville 1999). Continuous evaluations of network performance have determined a stroke DE of ~98% for CGLSS-II, with most of the missed detections due to high current strokes that saturate the local network of sensors (Ward *et al.* 2008b). Table 1 presents derived 95% confidence location accuracy metrics for CGLSS-II. Re-evaluations of location accuracy had to be conducted since a lightning strike destroyed sensor #2 (Melbourne) on 26 July 2009. Sensor #6 was re-located to the sensor #2 site and the new five-sensor configuration was established on 11 August 2009. In addition to this change, vendor configuration software in CGLSS-II was reset on 18 February 2010, which significantly improved the location accuracy. These strong performance metrics, combined with intense monitoring of the system by the 45 WS, strongly support its use as a valid comparison tool.

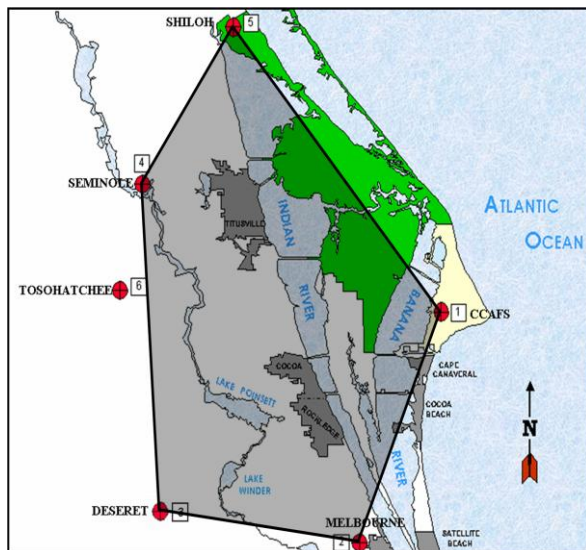


Figure 2. Locations of the six CGLSS-II sensors and the selected study region (shaded) for this project. Sensor #6 was not included in the study region since it was moved to replace sensor #2 (modified from Lambert *et al.* 2005).

Table 1. Derived 95% confidence CGLSS-II location accuracy metrics (Roeder 2010, personal communication).

Dates	95% Confidence CGLSS-II Location Accuracy
Pre 26 July 2009	693 m
11 August 2009 – 17 February 2010	981 m
Post 18 February 2010	567 m

Table 2 presents some similarities and differences between the USPLN and CGLSS-II networks. There are a couple key similarities that are pertinent to this study's methodology. First, both USPLN and CGLSS-II are stroke-based systems, meaning they can process locations for each individual stroke in a flash. This is useful since direct comparisons can be made without any possible biases due to flash algorithms. This is also quite different from many previous network comparisons, which have often been focused towards performance metrics for flashes. Second, both networks utilize the GPS time-of-arrival technique as a means of locating strokes. USPLN solely uses this technique, while CGLSS-II also occasionally utilizes magnetic direction finding when few sensors detect the stroke. The GPS timing allows for strong synchronization between both networks, which allows for a simple stroke matching procedure which is discussed in Section 2.4. A key difference for the networks is the sensor baseline (the average distance between sensors). The USPLN sensor baseline is clearly larger, but the baseline in Florida is actually smaller than what is seen across the CONUS. Therefore, some of the results in this study will need to be extrapolated since Florida is a well sampled region for the USPLN.

2. DATA AND METHODOLOGY

2.1. Data

The two main datasets collected were stroke data for the USPLN and CGLSS-II networks. CGLSS-II stroke data were acquired from two sources. First, data files were provided directly from the 45 WS for the period of 20 May 2008 to 31 August 2010. The files contained information for each stroke in a simple text format. CGLSS-II data were also extracted from the NASA Spaceport Weather Data Archives over the same period (NASA 2010). This source was consulted to fill in any possible gaps in the first set of files. A

Table 2. Listing of comparable key attributes for the CGLSS-II and USPLN networks.

Attribute	CGLSS-II	USPLN
Network Scale	Local	International
Sensor Baseline	~ 30 km	~ 250 km
Techniques	Magnetic Direction Finding Time of Arrival	Time of Arrival
GPS Technology	Yes	Yes
Flash/Stroke Reports	Stroke	Stroke

script was used to combine both files and effectively fill any gaps discovered in the files provided by the 45 WS. USPLN stroke data were provided by WSI in archived and real-time formats. The archive data was provided for a period spanning from 30 May 2004 to 30 April 2010. Over the summer of 2010, additional real-time data was collected from WSI through 31 August 2010. The acquired USPLN data were in a comma separated value (CSV) format, which was chosen as the primary format of this project due to its ease of use with statistical and graphical programs.

A third source of lightning data was also used with several case study examinations in this project. Data from the NASA/Air Force Four-Dimensional Lightning Surveillance System (4DLSS) were collected for the selected case studies. The 4DLSS is composed of the CGLSS-II and the second generation Lightning Detection and Ranging (LDAR-II) networks. LDAR-II is utilized to detect the individual leaders of a lightning stroke, allowing for detection of intra-cloud (IC) lightning. LDAR-I was previously used by Ward *et al.* (2008a) to classify small negative peak current (I_p) strokes as CG or IC strokes. In this study, LDAR-II is used to help classify USPLN strokes as IC or CG strokes. The large file sizes involved with the use of LDAR-II limited its use to individual case studies.

WMO (2009) explains that radar imagery can also be a useful tool in diagnosing network performance from a location standpoint. If strokes clearly lie well outside of a reflectivity echo associated with a convective cell, then they may be suspect. For this study, Melbourne (KMLB) WSR-88D composite reflectivity images were collected for the selected case studies from the National Climatic Data Center Radar Archives (NCDC 2010). Additional radar imagery support was provided by the CCAFS/KSC Warm-season Convective Wind Climatology database, which focuses on the KSC/CCAFS region (Plymouth State University 2010). To display the imagery, the Integrated Data Viewer (IDV) software was utilized (Unidata 2010). IDV was selected since

one can simultaneously plot radar images and point data. This was extremely useful since lightning data could easily be overlaid onto radar imagery for quick examination.

2.2. Temporal and Spatial Restrictions

The processor upgrade to CGLSS-II in 2008 limited the length of the period of study to 2008 and beyond, since previous to 2008 CGLSS-I was a flash-based system. Since CGLSS-II stroke data were available beginning on 20 May 2008, this was a logical choice to start the period of evaluation. The end of the evaluation period was selected to be 30 June 2010. While data were collected through 31 August 2010, inconsistencies in the USPLN data were discovered after 1 July 2010 and had to be flagged and not used for comparison. Thus, the selected period of study spans approximately two years, and includes two full summer periods.

The selected time period was further divided into sub-periods based on abrupt changes to the CGLSS-II network structure. Recall from Section 1 and Table 1 that the average performance of CGLSS-II changed when the network was reduced to five sensors and again when vendor configuration software was updated. Thus, three sub-periods were created based on these two key changes in the network. Sub-period I begins on 20 May 2008 and ends on 25 July 2009, one day before sensor #2 was damaged by lightning. Sub-period II begins on 11 August 2009, when the new five-sensor configuration was brought online, and ends on 17 February 2010. Finally, sub-period III begins on 18 February 2010, when the vendor configuration software was updated, and ends on 30 June 2010.

A definitive region of study also had to be selected. The locations of the CGLSS-II sensors were quite important in deciding this region. CGLSS-II performs best within the bounds of the network, which includes a significant portion of the KSC/CCAFS area. Outside of the network, performance degrades as one travels away from the network of sensors. With this in mind, it was

decided that the region of study would be confined to the region bound by the five-sensor configuration present during sub-periods II and III. The area is shown graphically in Figure 2. Sample size remained a relative non-issue due to the temporal scale of the project and the tendency for convection to form in this area due to mesoscale boundary interactions between the diurnal sea and river breezes (Ander *et al.* 2009).

2.3. Data Flagging and Quality Controls

The USPLN and CGLSS-II stroke datasets were converted into similar CSV formats. Information on the reported stroke time, location, and I_p strength were retained. During the conversion process, a number of quality controls and flags were implemented for the study. First, for both datasets, any test strokes were removed. Each format contained an indicator variable for a test stroke, which made it simple to eliminate any test strokes. Second, CGLSS-II strokes were only kept if their locations were within the region of interest defined in Figure 2. Third, CGLSS-II strokes were removed if they were weak positive strokes with I_p between 0 and +10 kA. Weak positive strokes have long been considered to be detected IC strokes (Roeder 2010, personal communication). The threshold of 10 kA has been decreasing with improved sensor sensitivity, but was retained at 10 kA for this study since it provides high confidence that a significant portion of IC strokes have been filtered. In contrast, weak negative strokes (I_p between -10 and 0 kA) were retained since previous studies have shown that CG strokes can have recorded I_p as low as -2 kA (Ward *et al.* 2008a). It is important to note that the last two quality controls were not applied to USPLN data. Restriction to the study region would bias the stroke matching procedure between the networks, particularly near the edges of the study region. Filtering of low current strokes would make an assumption about USPLN I_p calculation, and would bias stroke DE results and remove a set of possibly misclassified data.

While abrupt CGLSS-II structural changes were used to define sub-periods, changes in the USPLN network structure have not been included to this point. The fluid nature of USPLN expansion as part of the GLN and sensor outages made it difficult to define set sub-periods. A listing of sensor outages lasting 2+ hours for the nine USPLN Florida sensors (displayed in Figure 1) was provided by WSI (Krajewski 2010, personal communication). The outages were used to simply flag the stroke data from both networks with

two variables. The first was the number of Florida sensors offline, and the second was a code letter for the offline sensor location (e.g. if just the Clearwater sensor was down, the variables would be "1" and "C"). These flags were useful for data stratification in the performance analyses.

2.4. Stroke Correlation Procedure

With both stroke datasets converted and quality controlled, strokes that were detected by both networks had to be correlated, or matched. Previous studies indicated that GPS timing was very useful and allowed for a fairly simple correlation process. Ward *et al.* (2008b) considered CGLSS-I and NLDN events correlated if the CGLSS-I event occurred within 2 ms after the NLDN event. These were based on how each network determines the report time of each event. Gaffard *et al.* (2008) concluded that the time difference between correlated strokes from the ATDNet and Meteo-France networks was on the order of microseconds, with few producing differences higher than ± 1 ms. Both of those networks are stroke-detection networks with GPS timing, as are CGLSS-II and USPLN. In addition, exploratory analysis for this study revealed that most matches occurred when the time difference was less than ± 3 ms. Therefore, using the exploratory analysis, previous study conclusions, and a conservative approach, USPLN strokes were first considered correlated with CGLSS-II strokes if the occurrence time difference was less than ± 3 ms.

It was evident that several previous studies included a distance threshold as well. Previous research using photometry concluded that the distance between correlated stroke locations was typically less than 10 km (Thottappillil *et al.* 1992). Additional studies have concluded a distance of 12 km (Flinn *et al.* 2010). The distance between the USPLN and CGLSS-II reported locations was already being calculated in the correlation procedure for use with the location accuracy analysis. This was done using the Great Circle Distance Formula, provided by Lambert and Roeder (2008). It was decided that stroke matches were only kept if the distance between the locations was less than 15 km. This threshold agreed well with the conclusions from previous studies, and with exploratory analysis which revealed less than 2% of stroke matches with higher distances than 15 km.

Following the correlation procedure, two quality control checks were implemented. First, repeated use of strokes for correlations needed to

be filtered, so the match closest temporally or spatially (if the time difference was the same) was retained. Second, manual filtering was conducted to simply check for any suspicious pairs that happened to pass the time and distance thresholds. Additional variables were used (e.g. highly opposite I_p readings or opposite polarities) to determine if stroke pairs were suspicious. The manual filtering was highly conservative, since proof such as video evidence was not available.

2.5. Stroke Detection Efficiency

2.5.1. CGLSS-II Peak Current Variation

The first performance metric often examined when evaluating lightning networks is DE. Stroke DE was evaluated in this project since direct stroke to stroke comparisons could be made. It has been well documented (Gaffard *et al.* 2008; Ward *et al.* 2008b; WMO 2009) that network stroke DE varies as a function of I_p , with stroke DE often increasing as the peak current magnitude $|I_p|$ increases. CGLSS-II I_p calculations are derived from range-normalized signal strength, which means that strokes that produce less of a signal at the sensors receive lower $|I_p|$ values (Flinn *et al.* 2010).

The strength of the relationship between USPLN stroke DE and CGLSS-II $|I_p|$ was first checked using logistic regression (LR). LR uses a two-class binomial response based on one or multiple explanatory variables. For each stroke, the response is detection (or no detection) by the USPLN and the explanatory variable is the CGLSS-II $|I_p|$ parameter. Files were created that contain these two variables along with the outage flag variables for all strokes in the dataset. The statistical and graphics programming environment, R, was used to perform the LR analysis (R Development Core Team 2010). A script was created that generated LR models for the dataset stratified by the number of offline USPLN Florida sensors. Therefore, one LR model was made for data when zero sensors were offline, another model when one sensor was offline, etc. Manning (2007) explained that the deviance output from a LR model in R could be used to formulate a pseudo-coefficient of determination (r^2). There are a number of equations available for calculating a pseudo- r^2 , and the following was suggested:

$$r^2 = 1 - \frac{\text{residual deviance}}{\text{null deviance}},$$

where the deviances are provided in the LR model output by R. The pseudo- r^2 was, and could be, interpreted similarly to a regular r^2 calculated for linear regression. Therefore, a higher pseudo- r^2 means a stronger relationship between USPLN stroke DE and CGLSS-II $|I_p|$.

LR models are rather difficult to visualize, so a method of discrete plotting along the lines of Ward *et al.* (2008b) was used to visualize any pattern in USPLN stroke DE by CGLSS-II $|I_p|$. For each discrete plot, 2 kA $|I_p|$ frequency bins that ranged from 0-50 kA were generated. It was assumed that CGLSS-II stroke DE was nearly 100% for all strokes with $|I_p|$ below 50 kA, since it had been shown that most strokes missed by CGLSS-II were high current strokes greater than 50 kA (Ward *et al.* 2008b). For each $|I_p|$ bin, the frequencies of CGLSS-II strokes and those detected by the USPLN were counted. For example, if 200 strokes had $|I_p|$ between 18-20 kA, and 75 of those strokes were detected by the USPLN, then the frequencies for that $|I_p|$ bin were 200 and 75, respectively. In addition to the frequency plots, USPLN stroke DE curves as a function of $|I_p|$ were generated by simply calculating the stroke DE for each $|I_p|$ bin. Error bars were also included in the DE curve by assuming a normalized binomial distribution, so the standard deviation was plotted using the following equation:

$$\sigma = \sqrt{\frac{DE(1-DE)}{CGLSS}},$$

where DE is the stroke DE for the selected $|I_p|$ bin and CGLSS is the frequency of CGLSS-II strokes for that same $|I_p|$ bin.

It was expected that a similar relationship to those established in previous studies would be seen. The USPLN would excel at detecting higher current strokes with most of the missed detections occurring in the lower $|I_p|$ bins, particularly below 10 kA. It was also expected that stroke DE would improve with time and decrease as the number of offline USPLN sensors increased. An increase in time would be attributed to continued improvements with USPLN structure and software. A decrease with sensor outages would be due to an affected sensor baseline across Florida, leaving fewer sensors to detect strokes.

2.5.2. Stroke Rate Variation

In addition to the commonly-used I_p variation in stroke DE, variation based on spatial

and temporal frequencies of strokes was also conducted. In theory, it would make sense to believe that a network may perform better when few strokes are occurring versus when many strokes are occurring in the same area within a short amount of time.

A grid within the study region was selected to determine CGLSS-II stroke rates (in strokes $\text{km}^{-2} \text{hr}^{-1}$) during the period of study. Each box in the 30-box grid (seen in Figure 3) was 0.5 degrees latitude by 0.5 degrees longitude, producing a box area of roughly 27 km^2 . Data selected for this analysis occurred only when all USPLN Florida sensors were online. This was done to filter out any possible bias due to sensor outages. For each selected hour, the frequency of CGLSS-II strokes was tallied for each grid box. CGLSS-II stroke rates were determined by simply dividing the tallies by the area of the grid box. Data were then aggregated for like stroke rates in order to calculate stroke DE values. For example, say a stroke rate of $5 \text{ strokes km}^{-2} \text{hr}^{-1}$ occurs 3 times throughout the period of study. A total of 67 CGLSS-II strokes occur during this rate, with 43 detected by the USPLN. Therefore, the calculated stroke DE for a stroke rate of $5 \text{ strokes km}^{-2} \text{hr}^{-1}$ would be $43/67$ or 0.642 .

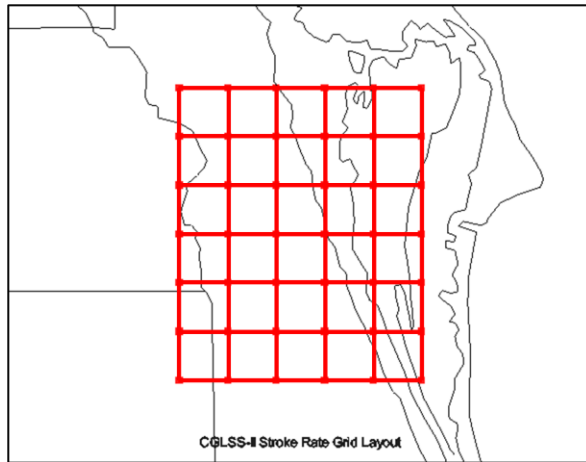


Figure 3. Selected grid for computing hourly CGLSS-II stroke rates. Each box is 0.5 degrees latitude by 0.5 degrees longitude, producing an area of $\sim 27 \text{ km}^2$.

A simple scatter-plot was generated using the resultant CGLSS-II stroke rates and their respective USPLN stroke DE calculations. It was expected that decrease in the USPLN stroke DE would be seen as the stroke rate increased. Therefore, as the amount of lightning activity

increases temporally and spatially, the USPLN detection ability would decrease.

2.6. USPLN Location Accuracy

2.6.1. Location Error

The second often-viewed performance metric is location accuracy. Specifically, this study evaluates the USPLN location error at 95% confidence. Recall that Table 1 contains 95% confidence CGLSS-II location errors, which serve as a location accuracy metric for CGLSS-II. It is possible, assuming independence between CGLSS-II and USPLN errors, to determine a 95% confidence USPLN location error using the CGLSS-II location accuracy metrics and the distance between matching stroke locations. By assuming independence, the total error (distance between stroke locations) is the addition of perpendicular error vectors (the CGLSS-II and USPLN location errors). The problem then becomes a simple application of the Pythagorean Theorem, and can be solved for the 95% confidence USPLN location error.

An R script was used to read in daily files of matching strokes, which were created from the correlation procedure. For each stroke pair, the distance between locations and the correct 95% confidence CGLSS-II location error were used to determine the 95% confidence USPLN location error through the procedure described above. The calculated location errors were stratified into groups by the number of offline USPLN sensors in order to determine variation as the sensor baseline changes. For each group, the median error was selected to represent average performance on that particular day. The variance of the location errors was also calculated to represent variation in performance on that particular day. A method of weighted-averaging was used to determine the average location error and variance for each sub-period, assuming independence. The following equations were applied:

$$\overline{LE} = w_1 LE_1 + w_2 LE_2 + \dots + w_n LE_n,$$

$$\overline{VAR} = w_1^2 VAR_1 + w_2^2 VAR_2 + \dots + w_n^2 VAR_n,$$

where LE was the daily USPLN location error, VAR was the variance, w was the selected weight, and the subscripts denoted different days. The weights were simply the ratio of the number of correlated strokes on the selected day over the

total number of correlated strokes during the sub-period. These weighted-average statistics were interpreted as the 95% confidence location accuracy and variation for the USPLN. It was expected that the location accuracy would improve with time, and weaken when USPLN sensors were offline.

2.6.2. Directional Error

Directional error was also examined to determine any biases for the USPLN within the region of study, and how these biases may change when selected USPLN sensors were offline. During the correlation procedure, the orientation of the USPLN location with respect to the CGLSS-II location (in degrees) was determined. A Perl script was used to create frequencies of correlated strokes using the calculated orientation for all strokes with distances greater than 3 km. The 3 km distance threshold was chosen to eliminate noise at lower distances. The frequencies were then displayed on histograms, with a histogram made for each different sensor combination seen in the dataset. Directional biases were then determined if substantial peaks were seen in the histograms at specific orientations. It was predicted that an east to northeast bias would be seen since the USPLN did not have a sensor located nearby on the eastern side of the study region.

2.7. Case Studies

Two case study days were selected using additional criteria for more detailed analyses. First, the case studies had to occur when all USPLN Florida sensors were online. Second, recent case studies were important, particularly in sub-periods II and III. This places more emphasis on recent USPLN performance. Third, at least 500 strokes must be reported by CGLSS-II to allow for sufficient sample size. Fourth, the case studies should span all levels of USPLN performance. Therefore, one day was selected where USPLN performance was excellent, and the other was selected when USPLN performance was poor.

The locations of all CGLSS-II and USPLN strokes within the region of interest were plotted on a position graph to provide a visual estimation of the performance of each network. Stroke DE and location accuracy metrics pertinent to each case study were also discussed to provide

additional detail and possible hypotheses for poor performance. Stroke DE was examined using the same discrete plot procedure as the overall analysis, while location accuracy was examined through the distribution of stroke distances between USPLN and CGLSS-II locations.

A specific subset of strokes that were researched in the case studies involved USPLN strokes within the study region that did not match CGLSS-II strokes. These were referred to as uncorrelated strokes. For each case study, 4DLSS data were acquired and converted into a format similar to the CGLSS-II and USPLN formats. An R script was used to generate time-height cross sections and position plots of all CGLSS-II and 4DLSS data within ± 0.5 s of the selected uncorrelated USPLN stroke. Plots were generated for each uncorrelated stroke and visually inspected to classify the stroke based on characteristics seen in the 4DLSS and CGLSS-II patterns. There were five possible categories for an uncorrelated stroke. First, the time-height cross section could have depicted a sequence of 4DLSS observations trailing from higher altitudes to the uncorrelated stroke location within a short amount of time. If the position plot revealed that both sets of observations were close to each other, then the uncorrelated stroke was classified as a true CG stroke that was detected by the USPLN and missed by CGLSS-II (if a CGLSS-II observation was not recorded). An example of a time-height and position plot of a true CG stroke is given in Figure 4. Second, the uncorrelated stroke could have been an IC stroke, which would have been evidenced by 4DLSS points located temporally and spatially with the uncorrelated stroke, but at high altitudes only. Two categories were created for this scenario. If the USPLN was correct in classifying it as an IC stroke, the uncorrelated stroke was placed in this category. The USPLN was capable of detecting some IC lightning as well as CG lightning, and IC strokes were denoted if the I_p variable was set to 0 kA for the stroke. An additional category was also created for misclassified IC strokes by the USPLN. Third, the uncorrelated stroke could be spatially or temporally separate from any 4DLSS or CGLSS-II activity. These strokes were categorized as "phantom" strokes. Fourth, an additional category of unclassified was also created if the 4DLSS and CGLSS-II data did not depict a clear category for the uncorrelated stroke examined. This was required since 4DLSS did not always clearly distinguish IC and CG strokes.

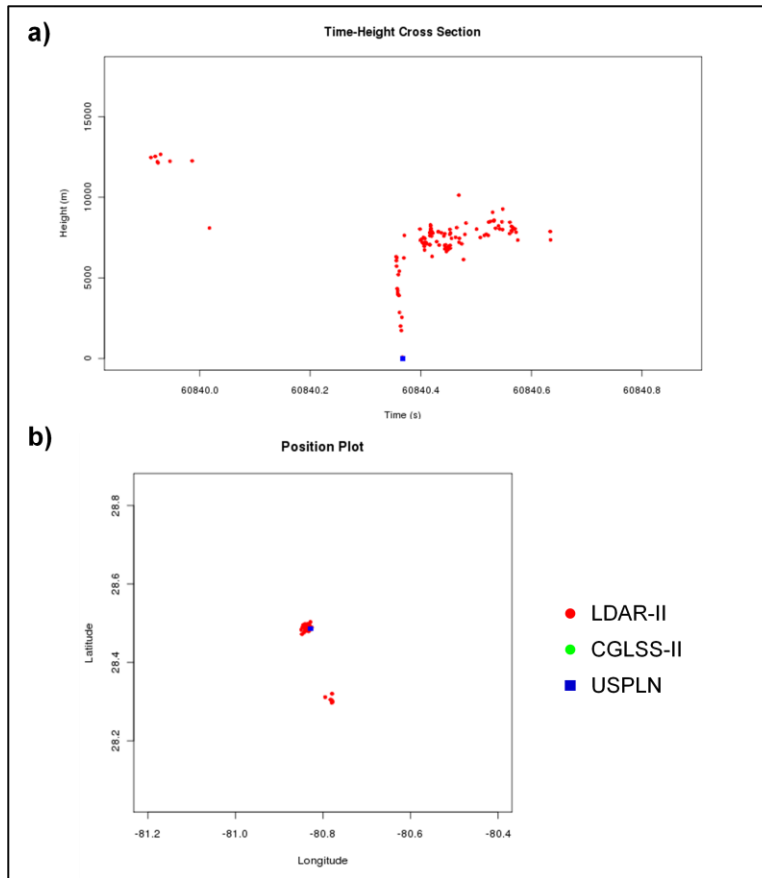


Figure 4. Example a) time height plot and b) position plot for a CG stroke detected by the USPLN but missed by CGLSS-II.

KMLB WSR-88D composite reflectivity imagery was utilized to examine the location of the “phantom” strokes compared to thunderstorm echoes. Considering these strokes were spatially or temporally separate from the 4DLSS data, there was reasonable cause to examine if they were also located well outside thunderstorm echo regions. Examination of these strokes was conducted using IDV to overlay the “phantom” stroke location onto the correct volume scan image. Some caution was applied when discussing these events since it is possible to generate CG lightning over portions of the thunderstorm anvil and outflow regions, where typical radar reflectivity values were small.

3. RESULTS

3.1. USPLN Sensor Outage Analyses

A quick analysis of USPLN sensor outage data was conducted to determine the number of striations required for the stroke DE and location

accuracy analyses. Outages of zero, one, or two USPLN Florida sensors were discovered during the period of study. No outages were recorded for about 65% of the total CGLSS-II stroke dataset. One sensor outages occurred for about 30% of the dataset, and the final 5% of the data occurred during two sensor outages. The most frequent sensor to be offline was the Clearwater sensor, which was out for about 26% of the dataset.

3.2. USPLN Stroke Detection Efficiency

3.2.1. Peak Current Variation Results

The results of the initial LR analysis revealed that there was some relationship between the CGLSS-II $|I_p|$ and detection by the USPLN. Three LR models were created after the data were striated into zero, one, and two-sensor outage datasets. Each LR model indicated that the CGLSS-II $|I_p|$ was a statistically significant predictor of detection, as evidence by z-test p-values very close to zero and well below the 0.05

threshold often used to establish statistical significance. The resultant pseudo- r^2 calculations for each model are displayed in Table 3. With a range of 0.32-0.46, clearly more factors than CGLSS-II $|I_p|$ were influencing whether detection by the USPLN occurs or not. However, it was interesting to see that the pseudo- r^2 changed very little between zero and one-sensor outages, yet increased dramatically when two-sensor outages occurred.

Table 3. The resultant slopes, intercepts, and pseudo- r^2 values for the logistic regression models created in the LR analysis.

Model	Slope	Intercept	Pseudo- r^2
Zero Offline Sensors	0.2110	-3.4456	0.3217
One Offline Sensor	0.2289	-3.6473	0.3391
Two Offline Sensors	0.2092	-5.7092	0.4523

The discrete plot analyses visually revealed some of the relationship seen in the LR analyses. Figures 5-7 display the frequencies of CGLSS-II strokes (red) and those detected by the USPLN (blue) for zero, one, and two-sensor outages, respectively. A clear problem was discovered with detecting low current strokes, regardless of the sensor outages. In particular, strokes with $|I_p|$ less than 14 kA do not produce stroke DE higher than 50% for any of the three sensor outage classes. It is hypothesized that the signal produced for lower current strokes may not be large enough to be detected by the USPLN sensors, which have a larger baseline than CGLSS-II. For higher current strokes, the USPLN stroke DE quickly increases. For zero sensor outages, the USPLN detected the majority of strokes with $|I_p|$ greater than 20 kA. Thus, the USPLN performs quite well in detecting the high current strokes, which perhaps may be more important to many customers.

A similar finding to the LR analysis was also discovered when plotting the stroke DE curves, which are shown in Figure 8. Note how the stroke DE curves for zero and one-sensor outages are almost identical for some $|I_p|$ bins. The similar nature of these curves supports the finding of similar pseudo- r^2 calculations for each dataset. Thus, it seems that detection of strokes does not change when one Florida USPLN sensor is offline. However, when two sensors are offline, note the drastic drop in detection for strokes with $|I_p|$ below 36 kA. Clearly the loss of an additional

sensor hampers the ability of the USPLN. These drastic changes in performance likely have to do with alterations to the USPLN sensor baseline, rather than the discrete number of sensor outages. One offline sensor does relatively little to significantly alter the sensor baseline in Florida, particularly when it is a sensor farther away from the study region (e.g. Clearwater). However, two sensors offline can dramatically change the sensor baseline. Thus, USPLN stroke DE performance is strongly impacted by the sensor baseline, and sensor outages should be considered when examining lightning data for a selected region.

An additional stroke DE curve plot is presented to show the temporal improvement in USPLN detection through the sub-periods. Figure 9 indicates that the detection of lower current strokes during sub-period I was a clear problem. However, the detection of lower current strokes did improve for sub-periods II and III, particularly for strokes with $|I_p|$ from 6-20 kA. An increased number of active sensors, instrument precision, and software are likely causes for the temporal increase in detection performance.

3.2.2. Stroke Rate Variation Results

The results of the CGLSS-II stroke rate analysis were quite interesting. The range of stroke rates calculated for each individual grid box was 0.03-11.63 strokes $\text{km}^{-2} \text{hr}^{-1}$. Figure 10 displays the resultant scatter-plot of calculated USPLN DE by CGLSS-II stroke rate, with a few large outliers removed. Outliers were removed in order to better view any possible trends in the results. A least-squares regression line was fit to the data, with subsequent equation and r^2 value located in the upper-right corner of the plot. Clearly, a strong relationship was not discovered in this analysis. The slope of the least-squares regression line was negative, which would suggest that there was some decrease in the USPLN stroke DE as the lightning activity increased. However, an r^2 value of less than 0.01 indicated a lack of a linear relationship between the two variables. Given the fairly random distribution of the observations in Figure 10, it seems that no clear relationship (e.g. exponential, logarithmic, etc.) could have been established between these two parameters. Thus, the USPLN stroke DE did not seem to typically increase or decrease greatly as the CGLSS-II stroke rate increased. Detection was similar regardless of whether many or few strokes were occurring over the region of study.

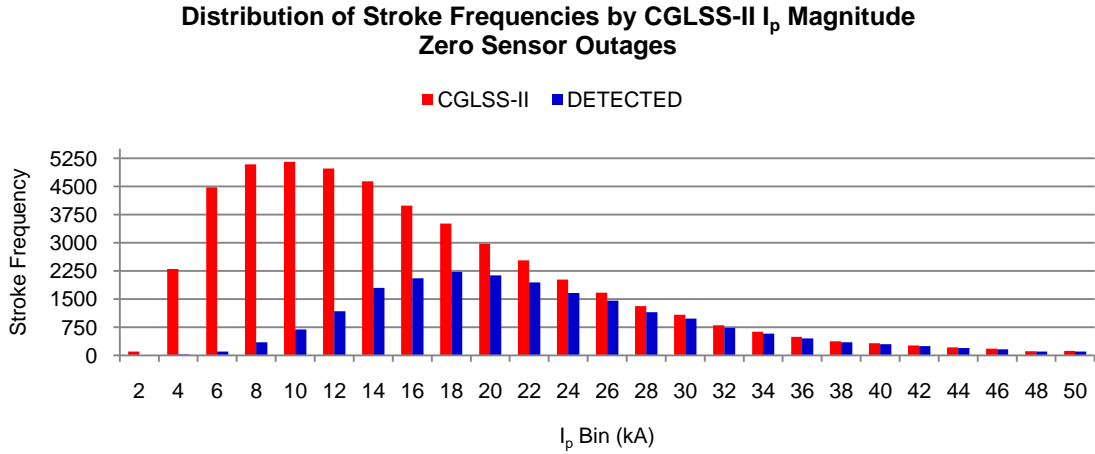


Figure 5. Distribution of CGLSS-II strokes by CGLSS-II $|I_p|$ are indicated by the red bars. The blue bars indicate the frequency of CGLSS-II strokes in each $|I_p|$ bin that were also detected by the USPLN. Stroke data for this plot occurred when all Florida USPLN sensors were online.

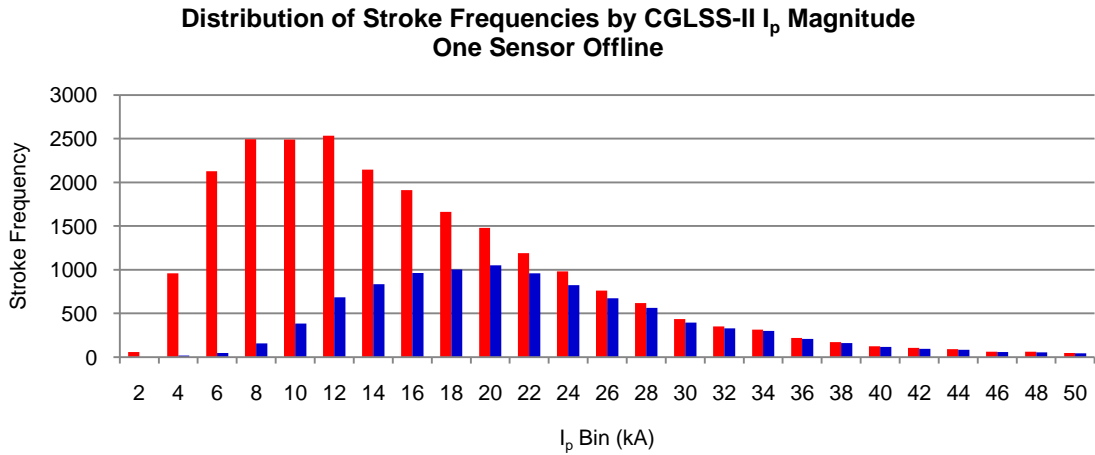


Figure 6. Same as Figure 5, except for stroke data when one USPLN sensor was offline.

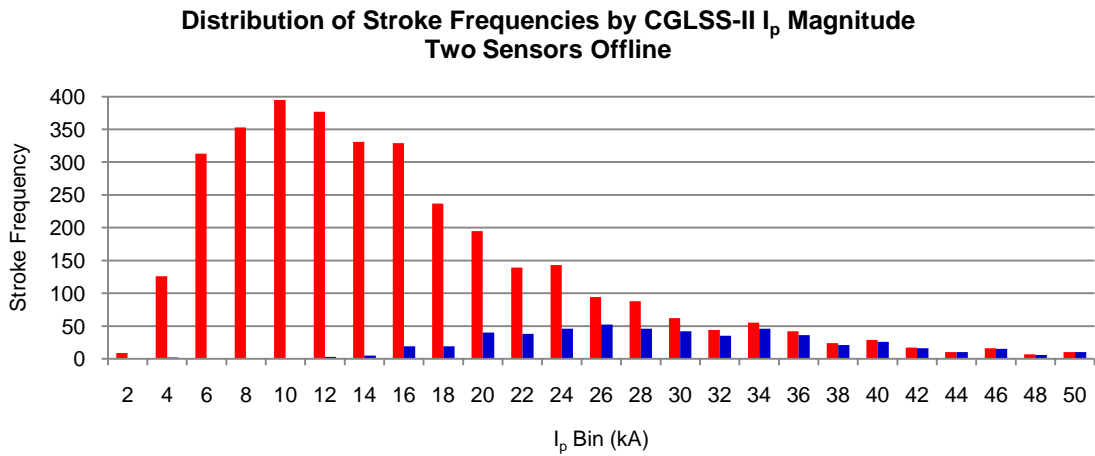


Figure 7. Same as Figure 5, except for stroke data when two USPLN sensors were offline.

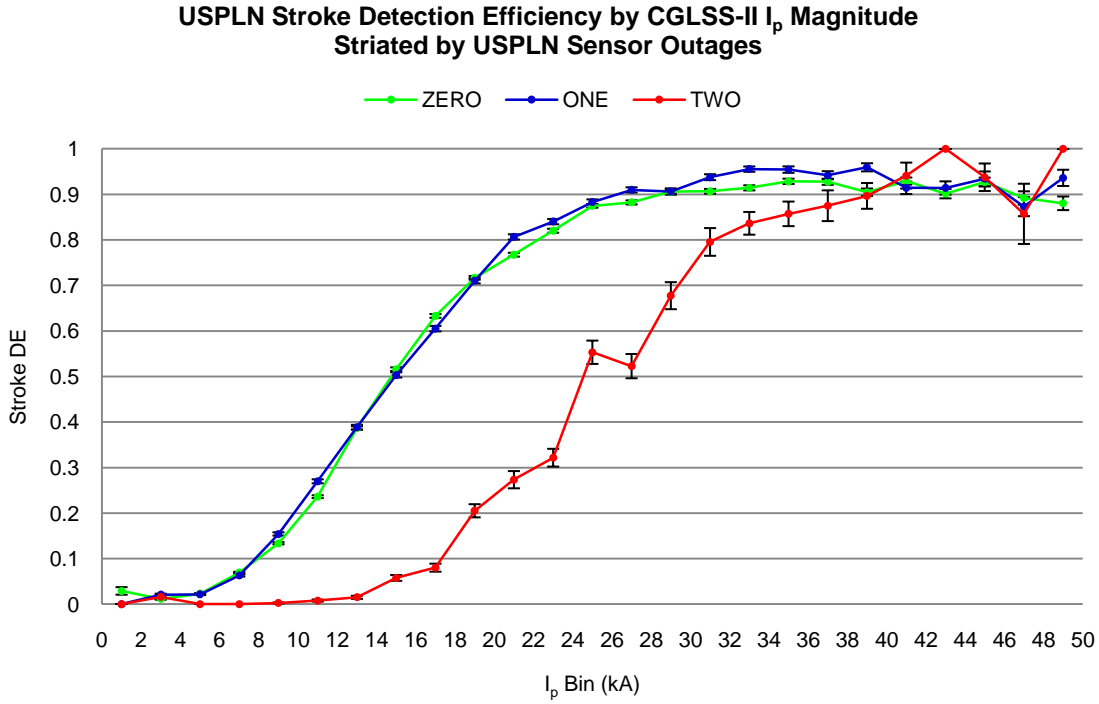


Figure 8. Derived stroke DE curves by CGLSS-II $|I_p|$ with error bars representing one standard deviation. Data for this plot were striated by the number of offline USPLN Florida sensors.

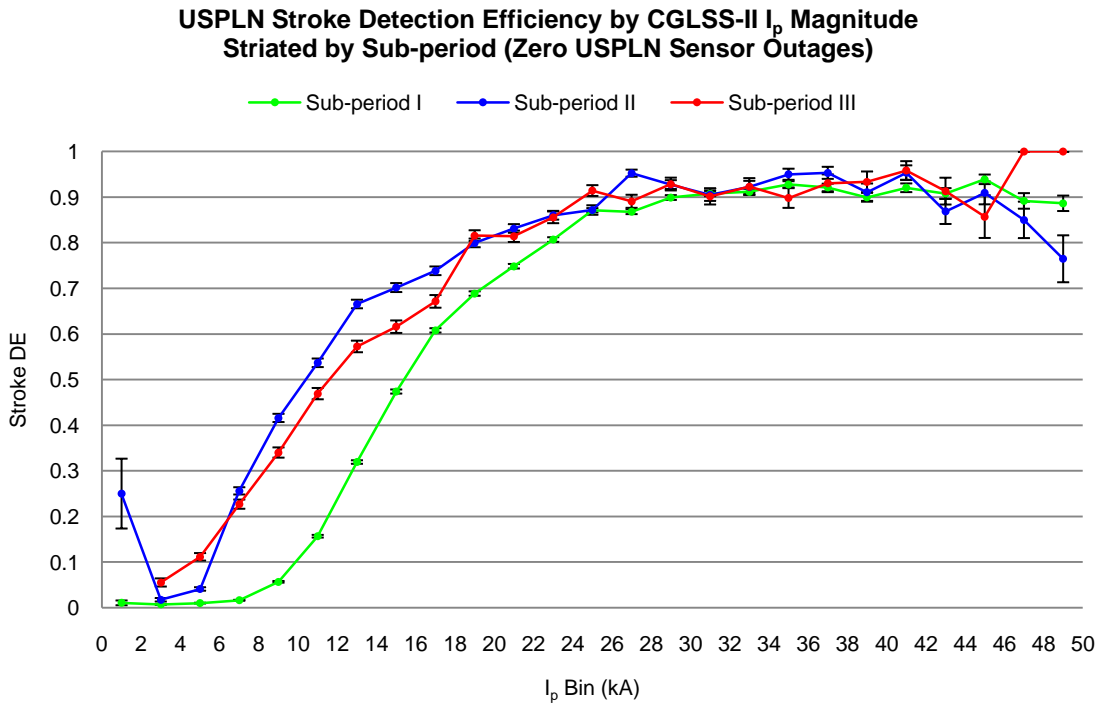


Figure 9. Derived stroke DE curves by CGLSS-II $|I_p|$ with appropriate error bars. Data for this plot were striated by sub-period and only occurred when all USPLN Florida Sensors were online.

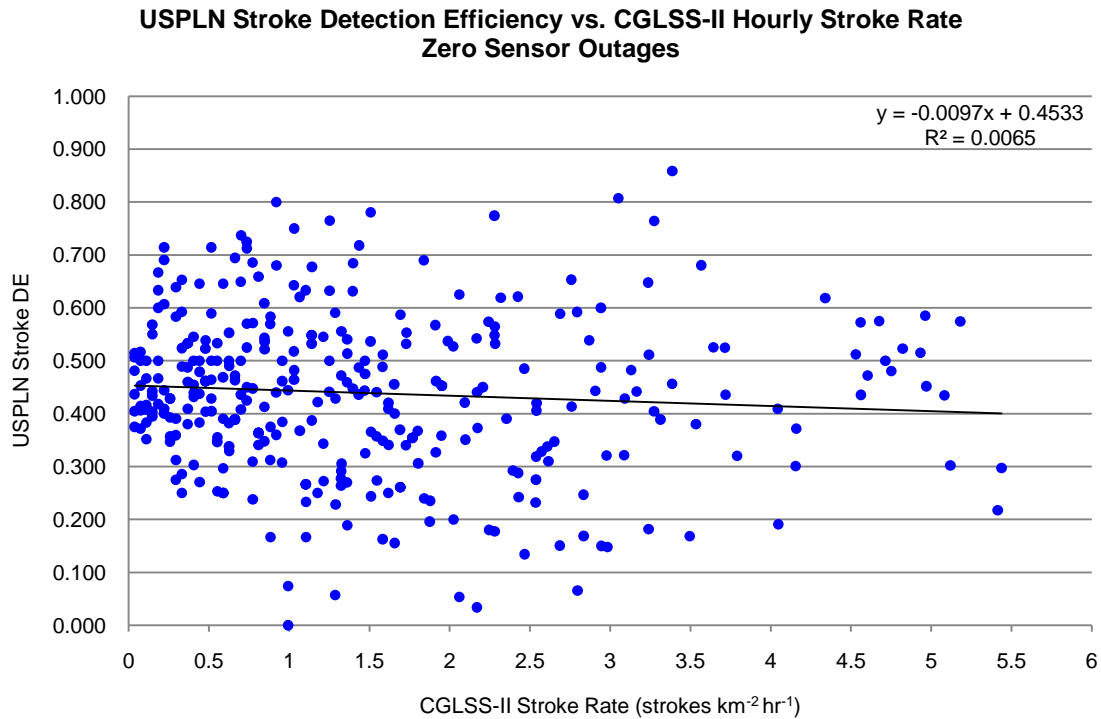


Figure 10. USPLN stroke DE versus CGLSS-II hourly stroke rate. A linear least-squares regression function was included, with subsequent equation and r^2 statistic displayed in the top right corner.

3.3. USPLN Stroke Location Accuracy

3.3.1. Location Error Results

Table 4 displays the weighted average 95% confidence USPLN location accuracy metrics for each sub-period and class of USPLN sensor outages, while Table 5 displays the respective variances. Recall that each metric is a weighted-average of the median daily values and daily variances (see section 2.6.1.). Note that similar patterns to what was seen in the I_p USPLN stroke DE analysis are also present here. A dramatic improvement in performance through the sub-periods is discovered when the network has no sensor outages for Florida. The most recent 95% confidence location accuracy stands at 626 m, which rivals the metrics calculated for CGLSS-II. This is exceptional considering the expanded sensor baseline of the USPLN. As seen before, note the lack of a significant decrease in performance when just one sensor is offline. In fact, during sub-period II the average metric improves, however this is somewhat nullified by a larger variance. This adds support to the fact that one offline sensor does little to change the baseline of the USPLN near the region of study. When two sensors are offline, the baseline is

clearly affected and so are the performance metrics. All two sensor outages occurred in sub-periods I and III, and a performance decrease is evident with large increases in the average 95% confidence USPLN location accuracy metrics and variances.

Table 4. USPLN 95% confidence location error results striated by sub-period and the number of offline USPLN Florida sensors. Median values for each day were used for the weighted average calculations.

Sensor Outages	Sub-Period I	Sub-Period II	Sub-Period III
Zero	1.410 km	1.190 km	0.626 km
One	1.475 km	0.844 km	0.891 km
Two	1.727 km	No Data	2.137 km

Table 5. USPLN location error variance results striated by sub-period and the number of offline USPLN Florida sensors. Variances for each day were used for the weighted variance calculations.

Sensor Outages	Sub-Period I	Sub-Period II	Sub-Period III
Zero	0.125 km	0.294 km	0.284 km
One	0.164 km	1.024 km	0.291 km
Two	0.890 km	No Data	14.075 km

3.3.2. Directional Error Results

The results for the directional error analysis reveal two large biases, one expected and the other unexpected. Figure 11 displays the histograms for each of the six prominent sensor outage combinations during the period of study. As expected, a clear northeast to east bias can be seen on all of the histograms. This is likely attributed to the lack of a close USPLN sensor to the east of the study region. The closest is located in the Bahamas, and is geographically south of the region as well. This affected the network's east-west line of sight over the study region, and little could be done to resolve this unless a sensor was placed to the east. The northeast bias occasionally shifted towards the north or east depending on which USPLN sensors were offline, which changed the sensor geometry around the region. An unexpected bias towards the southwest was also discovered in a number of histograms, but was most prominent when all Florida USPLN sensors are functioning. A possible explanation could be the semi-linear arrangement of the Melbourne, Moore Haven, and Naples sensors to the southwest of the study region. If these three sensors were primarily used in determining the location of a stroke, the error could have been subsequently greater since the time-of-arrival technique attempts to triangulate a region of possible solutions.

One should remember that the northeast and southwest biases discovered in this study apply to this region only. Biases for other portions of the network would be different due to different sensor geometries. However, the directional error study is still useful since it highlights the changes in directional biases when certain USPLN sensors were offline. This adds more importance to checking the status of the sensors when examining lightning activity since it clearly affects both detection and location of strokes.

3.4. Case Studies

3.4.1. 5 September 2009

There were a few outlier cases in sub-period II which prevented better average performance metrics for the USPLN. One of these cases was 5 September 2009, which produced weaker stroke DE and location accuracy metrics than what were calculated for the majority of the days. Figures 12a and 12b display the stroke locations for all CGLSS-II strokes and USPLN strokes within the region of study, respectively. A

clear eastward shift in the clusters of USPLN strokes can be seen compared to CGLSS-II. In addition, the distribution of strokes across the study area was more spread out for the USPLN compared to CGLSS-II, which primarily had two main clusters of strokes. An overall eastward bias was evident and it seemed to be fairly significant.

Figure 13 indicates that the USPLN had significant problems with detecting lower current strokes on 5 September 2009. A stroke DE of 50% is not consistently obtained until the $|I_p|$ increases above 22 kA. Stroke DE metrics above 25% are not reached until the $|I_p|$ increases above 16 kA. The stroke DE curve on this day (Figure 14) in general falls well below the curve derived for sub-period II on Figure 9. The location accuracy was also poor, as already evident in Figure 12b. The 95% confidence location accuracy for 5 September 2009 was found to be 3.770 km, well above the average 1.190 km for the entire sub-period. Figure 15 displays the distribution of distances between locations of matching USPLN and CGLSS-II strokes. A clear bimodal distribution is evident with peaks averaging near 1.5 and 5.5 km. This second peak at higher distances appears to be the culprit for the poor location accuracy, but no explanation appears feasible for why this occurred.

There were only 73 USPLN strokes within the study region that remained unmatched with CGLSS-II strokes. Table 6 shows the results of the 4DLSS identification analysis. There were 11 strokes identified as CG strokes missed by CGLSS-II. CGLSS-II detected 963 strokes on this day within the study region. Assuming all 963 were true CG strokes, then CGLSS-II missed only 1.1% of all CG strokes on this day, well within the ~2% concluded by Ward *et al.* (2008b). As expected, the majority of uncorrelated USPLN strokes were actually IC strokes. There were seven classified as "phantom" strokes, with a few of these having zero 4DLSS observations within ± 0.5 s of the recorded USPLN event time.

The radar analysis of the seven "phantom" strokes revealed that two occurred well outside the region encompassed by a convective cell. Figure 16 displays one of these two strokes, which was reported just southwest of Port Canaveral, FL while the closest storm cell was located northeast of KSC/CCAFS. These two strokes are deemed suspicious due to their lack of agreement with the radar imagery and the 4DLSS dataset. The other five "phantom" strokes were located within or near a storm cell, so the results for those strokes were inconclusive.

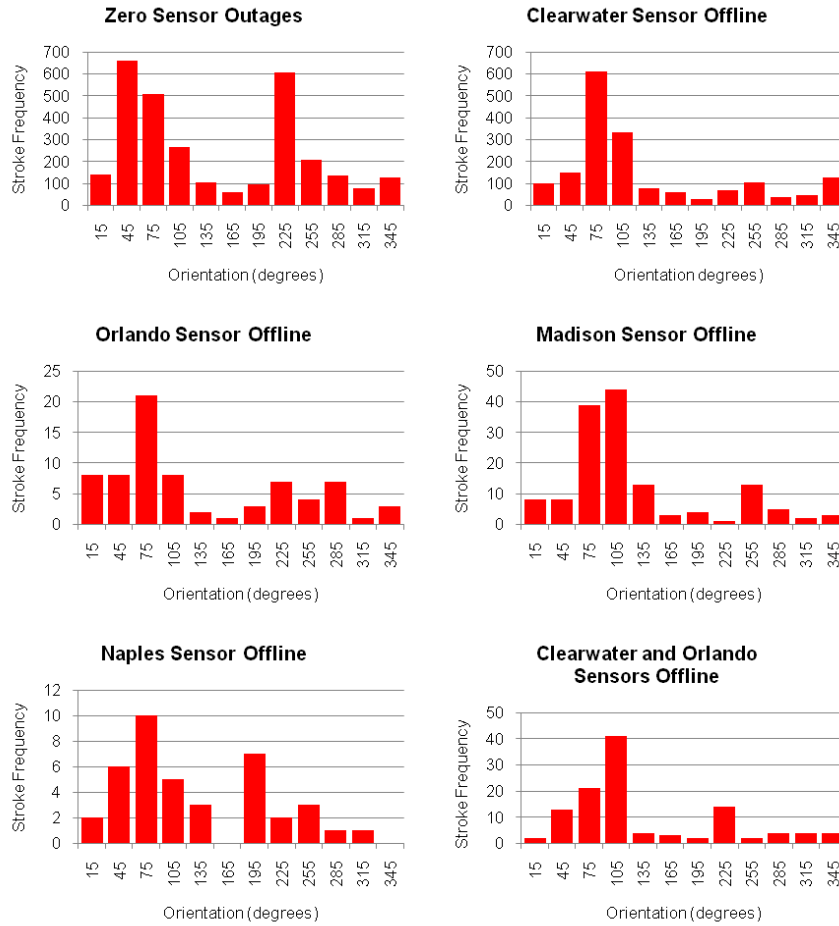


Figure 11. USPLN directional error histograms for each of the prominent sensor outage combinations. The x-axis refers to the orientation of the USPLN stroke location with respect to the CGLSS-II stroke location. Only matching stroke pairs with distances greater than 3 km were used in this analysis.

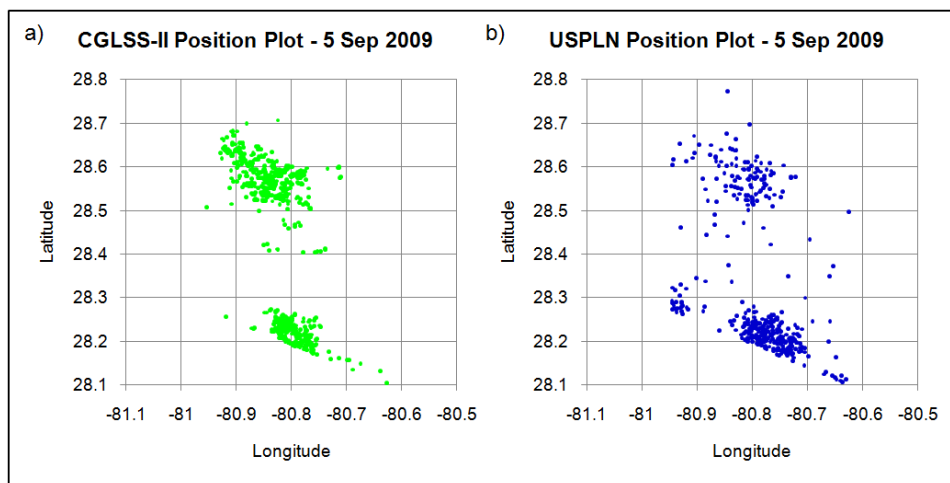


Figure 12. a) CGLSS-II stroke position plot and b) USPLN stroke position plot for 9 September 2009.

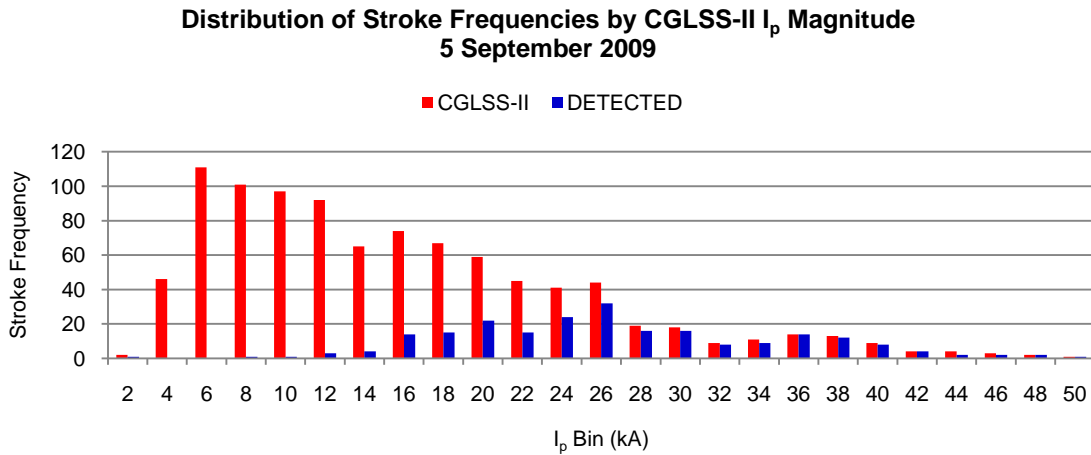


Figure 13. Same as Figure 5, except with stroke data from 9 September 2009.

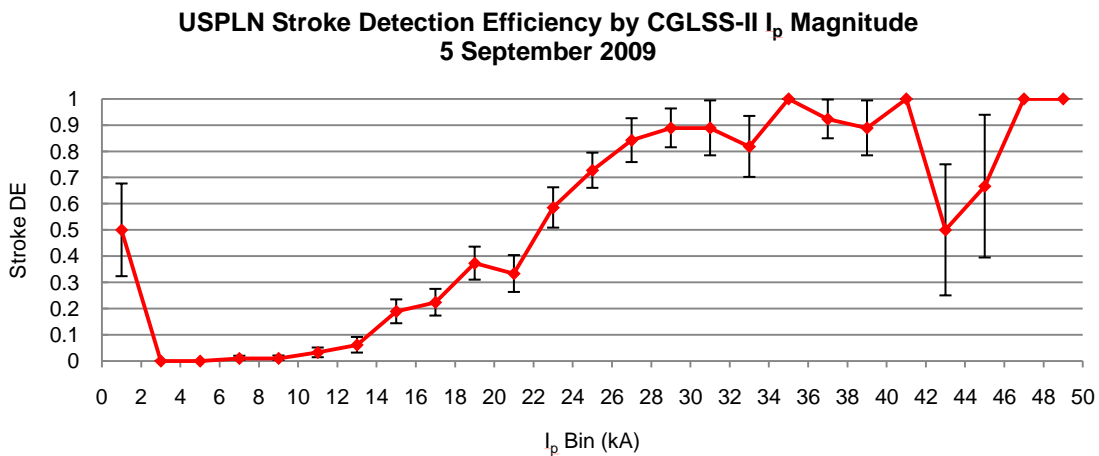


Figure 14. Derived USPLN stroke DE curve with error bars representing one standard deviation. Data for this figure are displayed in Figure 13.

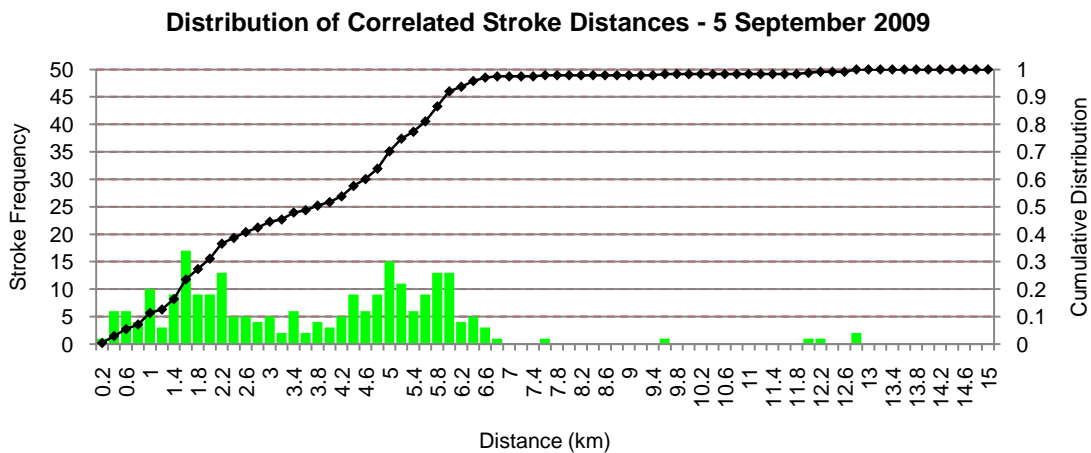


Figure 15. Distribution of distances between matching strokes for 5 September 2009. A cumulative distribution function was also included, with a secondary axis located on the right of the plot.

Table 6. Results of the 4DLSS analysis for uncorrelated USPLN strokes on 5 September 2009.

Category	Frequency	Percentage
CG stroke	11	15.07%
USPLN correctly classified IC stroke	6	8.22%
USPLN incorrectly classified IC stroke	40	54.79%
“Phantom” stroke	7	9.59%
Unclassified stroke	9	12.33%
Total unmatched USPLN strokes	73	100.00%

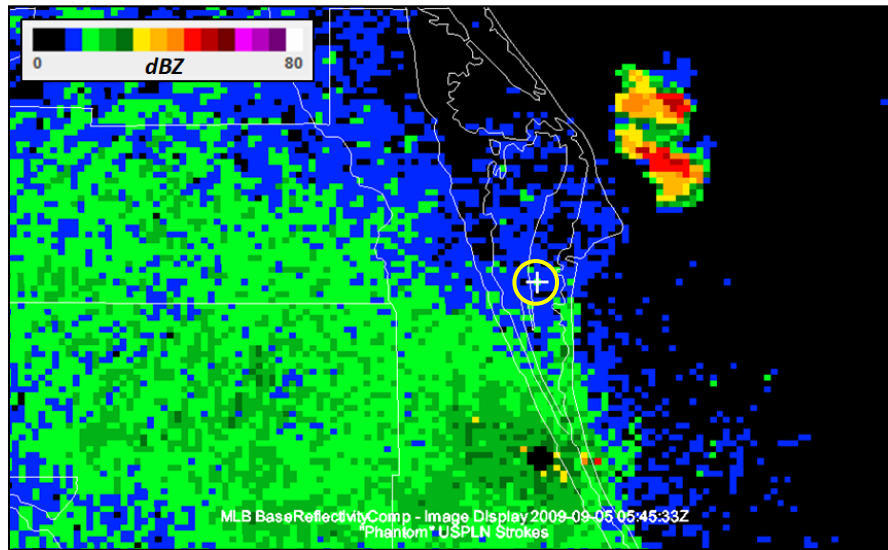


Figure 16. KMLB composite reflectivity image of a “phantom” stroke (white crosshairs outlined by a yellow circle) that occurred on 5 September 2009.

3.4.2. 15 June 2010

The second case study examined had much better performance metrics compared to 5 September 2009. Figures 17a and 17b indicate that both networks had similar locations of stroke clusters associated with individual storm cells, with the USPLN containing a few more stray strokes outside of the main clusters. The density of stroke locations also appears similar between the two networks, whereas a clear decrease in the number of strokes for the USPLN could be seen on 5 September 2009.

Figures 18 and 19 show that the stroke DE for 15 June 2010 was much better than the average DE for sub-period III. A stroke DE of 50% is already achieved for $|I_p|$ higher than 8 kA. A stroke DE of 90% is obtained at $|I_p|$ higher than 16 kA. Considering that 15 June 2010 occurred near the end of the evaluated study period, this is an excellent sign for USPLN performance and a clear improvement. The location accuracy was also excellent, with a 95% confidence location

accuracy metric of 576 m. The distribution of stroke distances in Figure 20 displays a clear peak between 200-600 m, with no secondary peak noted.

There were 348 USPLN strokes that were uncorrelated within the study region. The 4DLSS identification analysis results are displayed in Table 7. There were 42 strokes identified as CG strokes missed by CGLSS-II. There were 869 strokes detected by CGLSS-II on 15 June 2010, so CGLSS-II missed 4.6% of CG strokes on this day. This percentage was much higher than what was discovered on 5 September 2009 and what Ward *et al.* (2008b) concluded. Most of the uncorrelated strokes were still classified as IC strokes. There were five “phantom” strokes, but they did contain some 4DLSS observations on their respective time-height and position plots. Examination of these strokes with radar imagery revealed that all five strokes were located in or around a thunderstorm echo. Figure 21 depicts one of the “phantom” strokes from 15 June 2010.

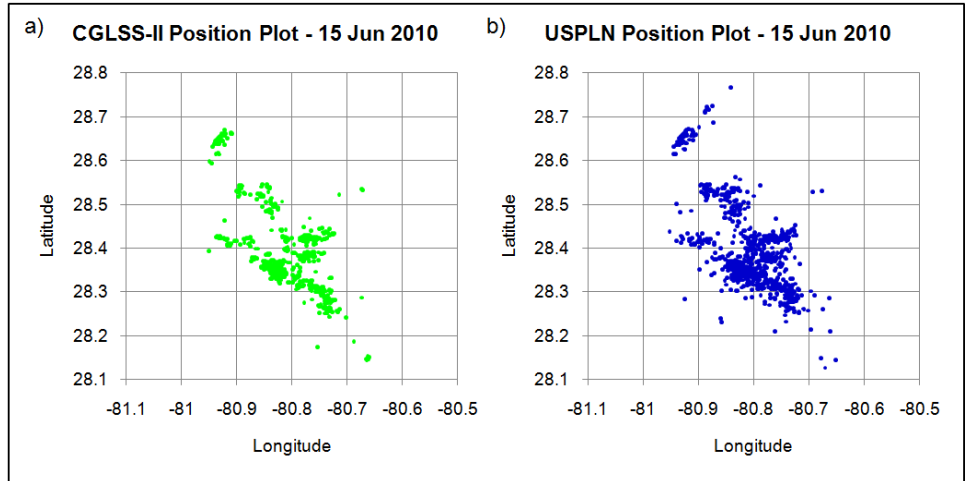


Figure 17. a) CGLSS-II stroke position plot and b) USPLN stroke position plot for 15 June 2010.

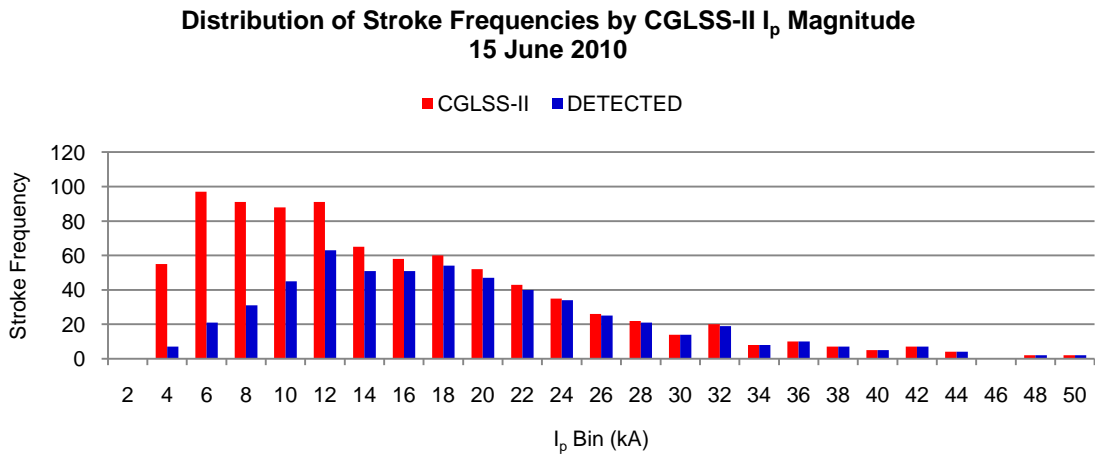


Figure 18. Same as Figure 5, except with stroke data from 15 June 2010.

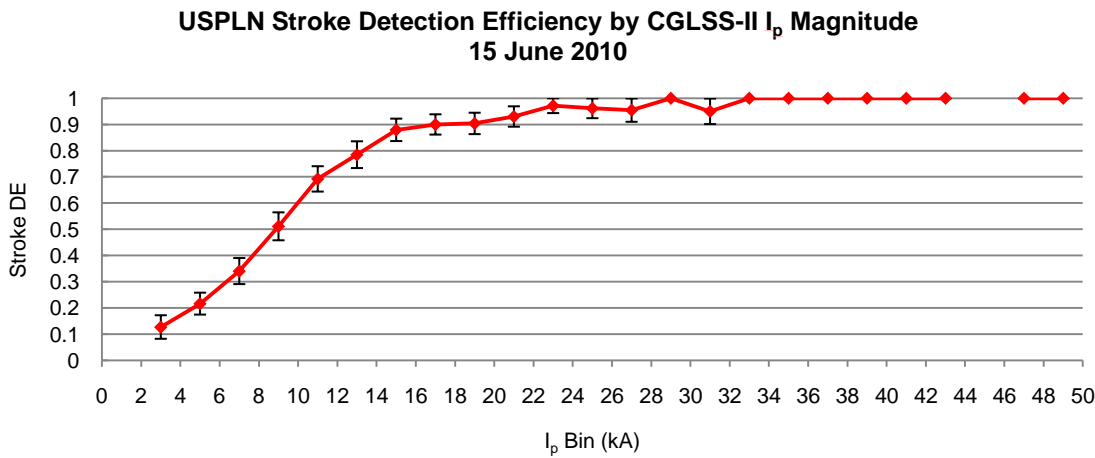


Figure 19. Derived USPLN stroke DE curve with error bars representing one standard deviation. Data for this figure are displayed in Figure 18.

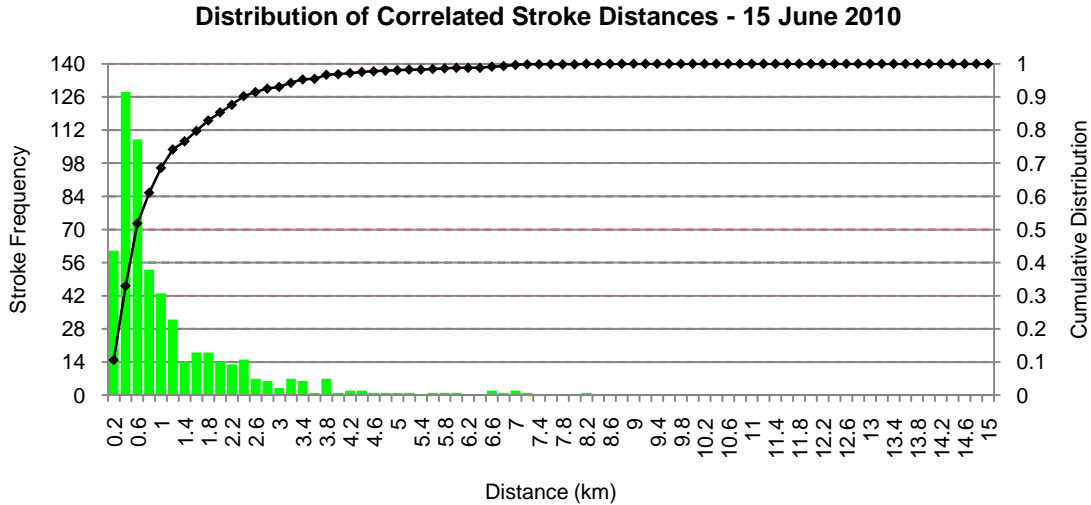


Figure 20. Distribution of distances between matching strokes for 15 June 2010.

Table 7. Results of the 4DLSS analysis for uncorrelated USPLN strokes on 15 June 2010.

Category	Frequency	Percentage
CG stroke	42	12.07%
USPLN correctly classified IC stroke	56	16.09%
USPLN incorrectly classified IC stroke	192	55.17%
“Phantom” stroke	5	1.44%
Unclassified stroke	53	15.23%
Total unmatched USPLN strokes	348	100.00%

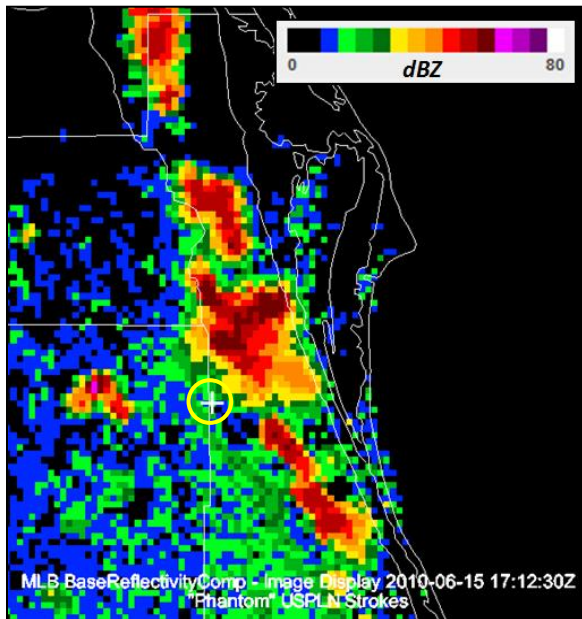


Figure 21. KMLB composite reflectivity image of a “phantom” stroke (white crosshairs outlined by a yellow circle) that occurred on 15 June 2010.

4. CONCLUSIONS AND DISCUSSION

It is clear that this study revealed several strengths and weaknesses for USPLN performance that were not discovered in the network simulation and fixed tower analyses. A clear improvement in performance was seen during the period of study. Stroke DE increased significantly for lower current strokes from sub-period I to sub-period II, with similar detection seen in sub-period III. Location accuracy also significantly improved with time, especially in sub-period III where a 95% confidence location accuracy of 626 m was calculated. The improved performance can likely be attributed to improved software upgrades in the system and the addition of sensors for the expanding GLN.

The stroke DE analyses revealed some relationship between CGLSS-II $|I_p|$ and detection by the USPLN. Weaker current strokes were the source for most of the missed detections by the USPLN, particularly those with $|I_p|$ below 10 kA. Detection for strokes with $|I_p|$ above 20 kA was excellent when the USPLN was operating with all Florida sensors online. Thus, it is difficult to use

one simple number to describe the detection performance of the USPLN. The correct performance metric to use may be heavily dependent on the needs of a customer. For example, if a customer is only concerned with stronger strokes, then a stroke DE should be calculated for only stronger current strokes. Based on the findings of this study, the stroke DE would be quite high for strong strokes. However, if weaker current strokes are also important, then the stroke DE would be much lower based on the findings in this study.

Both the stroke DE and location accuracy analyses indicated the importance of having a sufficient sensor baseline for optimal performance. Significant drops in the USPLN performance metrics were not seen when one USPLN sensor was offline, but were seen when two USPLN sensors were lost. The sensor baseline was greatly affected when two sensors were offline, especially considering the majority of two sensor outages included the Clearwater and Orlando sensors. This study also revealed that directional biases can be introduced based on the sensor geometry. Thus, outages of sensors nearby to an area of examination should be considered since a decrease in performance does occur when the sensor baseline is affected.

Analyses of unmatched USPLN strokes for the case studies using 4DLSS determined that a significant portion of these uncorrelated strokes were IC strokes classified as CG strokes by the USPLN. There were some CG strokes that USPLN detected and CGLSS-II missed, which are likely high current strokes that saturated the CGLSS-II network. CGLSS-II missed 1-5% of all CG strokes for the two case studies, which was fairly consistent with the ~2% determined by Ward *et al.* (2008b). A few “phantom” USPLN strokes were determined, but analysis with the radar imagery did little to justify if they really were spurious strokes.

It should be noted that in early December 2010 it was discovered through video confirmation of a lightning event that some of the CGLSS-II sensors required changes in configuration, which took place on 9 December 2010. This problem has been traced back to late June 2010. While this one event showcased a weakness in CGLSS-II performance, other known and evaluated events did take place during the period of study where CGLSS-II still retained excellent performance. Thus, it is not totally clear as to how this discovered problem may have slightly affected the results of this project. However, the data used in this study only extended to 30 June 2010 and

there was very little lightning activity in the study region during the latter part of June.

It is also important to note that all of the performance metrics calculated in this study are likely higher than what may be determined for other portions of the network. This is due to the increased USPLN sensor baseline across Florida compared to other regions of the CONUS. Thus, extrapolation of these results should be done if applying these metrics to other portions of the network, particularly in those regions where the spacing between sensors is greater.

5. FUTURE WORK

This study simply scratches the surface of what could be done when comparing the USPLN or any other lightning networks to each other. This study was the first to evaluate USPLN performance over a long-term period, so additional studies and comparisons should be conducted. Additional case studies comparing 4DLSS to the USPLN should be done to further expand the results discovered in the 4DLSS analyses in this study. Comparisons to other local detection networks in different regions of the country could be done to determine how performance may vary over other regions. Of course, a nationwide comparison could be done using another large-scale detection network, such as the NLDN. Location accuracy and stroke DE could be conducted in a similar manner to this study, using known and tested performance metrics from the comparative network.

More investigation should be done involving the lack of detection of lower current strokes by the USPLN. It is likely that a percentage of these lower current strokes detected by CGLSS-II are actually IC strokes, but determining what that percentage is and which ones are difficult matters. For this study, a conservative approach was taken by only eliminating weak positive current strokes, while retaining all weak negative strokes. The magnitude of the 4DLSS dataset limited its use to the case studies, so for a short-term study, 4DLSS could be used to help eliminate some of these IC strokes. However, 4DLSS is not full-proof either, as evidenced in the case studies where some of the USPLN strokes could not be classified. CG strokes that occur in pre-existing channels are also an issue. It would be interesting to compare performance metrics (particularly stroke DE) for sub-period III using an additional CGLSS-II dataset where strokes were eliminated based on classification using 4DLSS to see if the lack of

detection was overdone due to additional IC strokes in the dataset.

Analysis of peak current accuracy for the USPLN could also be done in the future. Peak current accuracy is often used as a third performance metric, but its importance is heavily dependent on the customer. This study was focused on detection and location, since most customers are primarily concerned about where and when strokes hit. However, peak current analyses could also be included for future studies.

Perhaps the biggest push for an additional analysis will occur once both networks are upgraded. At the present time, new sensors for the USPLN are being tested by TOA Systems, Inc. for future implementation. CGLSS-II is also working towards eventually getting new sensors and re-establishing the six-sensor configuration that was previously in place. Once these are finished, a new analysis could be done to determine if performance has increased due to the new sensors.

6. ACKNOWLEDGEMENTS

The authors would like to thank WSI Corporation for their support and primary funding of this project. The NASA New Hampshire Space Grant Consortium also provided some funding for logistical support. We would also like to specifically thank the 45th Weather Squadron and the NASA Applied Meteorology Unit (AMU), who provided CGLSS-II data and guidance for this research while working at CCAFS during the summer of 2010. Additionally, we would like to thank NCDC for providing archived radar data for this study.

7. REFERENCES

Ander, C.J., A.J. Frumkin, J.P. Koermer, and W.P. Roeder, 2009: Study of sea-breeze interactions which can produce strong warm-season convective winds in the Cape Canaveral area, *Joint session of the 16th Conf. on Air-Sea Interaction and the 8th Conf. on Coastal Atmospheric and Oceanic Prediction and Processes*, Amer. Met. Soc., Phoenix, AZ.

Boyd, B.F., W.P. Roeder, D. Hajek, and M.B. Wilson, 2005: Installation, upgrade, and evaluation of a short-baseline cloud-to-ground lightning surveillance system in support of space launch operations. *1st Conf. on Meteorological Applications of Lightning Data*, Amer. Met. Soc., San Diego, CA, P2.4.

Flinn, F.C., W.P. Roeder, D.F. Pinter, S.M. Holmquist, M.D. Buchanan, T.M. McNamara, M. McAleenan, K.A. Winters, P.S. Gemmer, M.E. Fitzpatrick, and R.D. Gonzalez, 2010: Recent improvements in lightning reporting at 45th Weather Squadron. *Extended Abstracts, 14th Conf. on Aviation, Range and Aerospace Meteorology*, Amer. Met. Soc., Atlanta, GA, 7.3.

Gaffard, C., J. Nash, N. Atkinson, A. Bennett, G. Callaghan, E. Hibbett, P. Taylor, M. Turp, and W. Schulz, 2008: Observing lightning around the globe from the surface. *20th International Lightning Detection Conference*, Royal Met. Soc., Tucson, AZ, 12 pp.

Huffines, G. R., and R. E. Orville, 1999: Lightning ground flash density and thunderstorm duration in the continental United States: 1989-96. *Journal of Applied Meteorology*, **38**, 1013-1019.

Lambert, W.C., and W.P. Roeder, 2008: Update to the lightning probability forecast equations at Kennedy Space Center/Cape Canaveral Air Force Station, Florida. *20th International Lightning Detection Conference*, Royal Met. Soc., Tucson, AZ, 16 pp.

_____, M. Wheeler, and W. Roeder, 2005: Objective lightning forecasting at Kennedy Space Center and Cape Canaveral Air Force Station using Cloud-to-Ground Lightning Surveillance System data. *Extended Abstracts, 1st Conf. on Meteorological Applications of Lightning Data*, Amer. Met. Soc., San Diego, CA, 4.1.

Manning, C., cited 2010: Logistic Regression (with R). [Available online at <http://nlp.stanford.edu/~manning/courses/ling289/logistic.pdf>.]

McNamara, T.M., W.P. Roeder, and F.J. Merceret, 2010: The 2009 update to the Lightning Launch Commit Criteria. *Extended Abstracts, 14th Conf. on Aviation, Range and Aerospace Meteorology*, Amer. Met. Soc., Atlanta, GA, 469.

NASA, cited 2010: 4DLSS NASA Spaceport Weather Data Archives. [Available online at <ftp://trmm.ksc.nasa.gov/lightning/archives/4DLSS/>.]

NCDC, cited 2010: NCDC Radar Resources. [Available online at <http://www.ncdc.noaa.gov/oa/radar/radarresources.html>.]

Neilley, P.P., and R.B. Bent, 2009: An overview of the United States Precision Lightning Network (USPLN). *4th Conf. on Meteorological Applications of Lightning Data*, Amer. Met. Soc., Phoenix, AZ, 4.2.

- Plymouth State University, cited 2010:
CCAFS/KSC Warm-Season Convective Wind
Climatology. [Available online at
http://vortex.plymouth.edu/conv_winds.]
- R Development Core Team, 2010: R Foundation
for Statistical Computing. Vienna, Austria.
[Available online at <http://www.rproject.org>.]
- Thottappillil, R., V.A. Rakov, M.A. Uman, W.H.
Beasley, M.J. Master, and D.V. Shelukhin,
1992: Lightning subsequent-stroke electric
field peak greater than the first stroke peak
and multiple ground terminations. *J.
Geophys. Res.*, **97** (D7), 7503-7509,
doi:10.1029/92JD00557.
- Unidata, cited 2010: Integrated Data Viewer (IDV).
[Available online at [http://www.unidata.
ucar.edu/software/idv/](http://www.unidata.
ucar.edu/software/idv/).]
- Ward, J.G., K.L. Cummins, E.P. Krider, 2008a:
Classification of small negative lightning
reports at the KSC-ER. *20th International
Lightning Detection Conference*, Royal Met.
Soc., Tucson, AZ, 13 pp.
- Ward, J.G., K.L. Cummins, E.P. Krider, 2008b:
Comparison of the KSC-ER Cloud-to-Ground
Lightning Surveillance System (CGLSS) and
the U.S. National Lightning Detection
NetworkTM (NLDN). *20th International
Lightning Detection Conference*, Royal Met.
Soc., Tucson, AZ, 7 pp.
- WMO, 2009: Remote sensing systems (such as
GPS, microwave, and infrared radiometers,
lidars, etc.) for their use in WIGOS: Update of
the CIMO Guide – Locating the source of
lightning events. CBS-CIMO Remote
Sensing Doc. 4.1(3), 14 pp. [Available online
at [http://www.wmo.int/pages/prog/www/
IMOP/meetings/Upper-Air/ET-RSUATT-2/
Doc-4-1-3.doc](http://www.wmo.int/pages/prog/www/
IMOP/meetings/Upper-Air/ET-RSUATT-2/
Doc-4-1-3.doc).]